ResearchGate

See discussions, stats, and author profiles for this publication at: https://www.researchgate.net/publication/257445795

Conformation and Orientation of Phospholipid Molecule in Pure Phospholipid Monolayer During Compressing

ARTICLE *in* CHINESE JOURNAL OF CHEMICAL ENGINEERING · FEBRUARY 2013

Impact Factor: 1.1 · DOI: 10.1016/S1004-9541(13)60456-5

READS

18

4 AUTHORS, INCLUDING:

Xuechao Gao

University of Queensland

7 PUBLICATIONS **35** CITATIONS

SEE PROFILE

Available from: Xuechao Gao

Retrieved on: 28 January 2016

BIOTECHNOLOGY AND BIOENGINEERING
Chinese Journal of Chemical Engineering, **21**(2) 177—184 (2013)
DOI: 10.1016/S1004-9541(13)60456-5

Conformation and Orientation of Phospholipid Molecule in Pure Phospholipid Monolayer During Compressing*

XUE Weilan (薛为岚), **WANG Dan** (王丹), **ZENG Zuoxiang** (曾作祥)** and **GAO Xuechao** (高雪超)
Institute of Chemical Engineering, East China University of Science and Technology, Shanghai 200237, China

Abstract On the basis of energy conservation law and surface pressure isotherm, the conformation energy changes of dipalmitoylphosphatidylcholine (DPPC) and dipalmitoylphosphatidylglycerol (DPPG) in pure phospholipid monolayer at the air/water interface during compression are derived. The optimized conformations of phospholipids at absolute freedom state are simulated by Gaussian 98 software. Based on following assumptions: (1) the conformation energy change is mainly caused by the rotation of one special bond; (2) the atoms of glycerol near the water surface are active; (3) the rotation is motivated by hydrogen-bond action; (4) the rotation of bond is inertial, one simplified track of conformational change is suggested and the conformations of DPPC and DPPG at different states are determined by the plots of conformation energy change *vs*. dihedral angle. The thickness of the simulated phospholipid monolayer is consistent with published experimental result. According to molecular areas at different states, the molecular orientations in the compressing process are also developed.
Keywords dipalmitoylphosphatidylcholine, dipalmitoylphosphatidylglycerol, phospholipid monolayer, conformation, orientation

1 INTRODUCTION

Phospholipid monolayers play a major role in the biological processes by regulating surface tension at the air/alveolar interface, and thus facilitate the breathing and prevent alveolar collapse [1, 2]. The lipids mainly include phosphatidylcholine (PC) and phosphatidylglycerol (PG). Dipalmitoylphosphatidylcholine (DPPC) is the most abundant and the most surface-active dipalmitoylphosphatidylglycerol (DPPG) can increase the fluidity of lipid film and facilitate DPPC re-spreading in monolayers [3].

Understanding the conformation and orientation of phospholipid molecules at the air/water interface during compression will help us to understand the breathing process. Many experimental techniques and methods were employed to derive conformational and orientational information including neutron reflection to study the chain tilt angle of monolayer [4], infrared and Raman spectroscopy to study the conformation of acyl chains [5, 6], sum frequency generation spectroscopy to study the conformation and orientation of hydrocarbon chains [7]. Recently, computer simulations were applied to investigate phospholipid monolayers [8–12]. Mohammad-Aghaie *et al*. [11] suggested that the choline head group tilt angle for DPPC undergoes little change during the liquid expanded (LE) to liquid condensed (LC) transition. The study focused on the lipid monolayer with large molecular area in LE and LC phases, without considering that with small molecular area approaching collapse phase.

The lowest phospholipid molecular area can not be smaller than the area of two fatty acyl chains (0.4 $nm^2 \cdot molecule^{-1}$) [13, 14]. It is true only for a single molecule, while the apparent area of molecules may be less than 0.4 $nm^2 \cdot molecule^{-1}$ for numerous molecules. More and more data for the lipid monolayer with smaller molecular area (less than 0.4 $nm^2 \cdot molecule^{-1}$) were reported recently [15–20], providing the information to investigate the behavior of phospholipids with small area approaching collapse phase.

The objective of the present work is to determine the conformation and orientation of DPPC and DPPG molecules during compressing process, particularly approaching the collapse phase. The corresponding single point energies are calculated by Gaussian 98 [21], the conformation of phospholipids at every state is determined, and the corresponding orientation at the interface is deduced.

2 CHARACTERISTIC STATES

For a pure phospholipid monolayer, in the compressing process, there are four characteristic states with the corresponding molecular area [22]: freedom state (A_f), liquid condensed (LC) state (A_{LC}), LC to collapse transition state (A_t), and collapse state (A_i). Before compressing, each molecule in freedom state occupies the biggest surface area A_f and its single point energy is the lowest, so the molecular conformation is the most stable. In the end of compression, the monolayer collapses. At this moment, each molecule reaches the lowest area A_i and its single point energy is the highest.

The average area per molecule (A) is a very important structural information for experiments [23]. For a pure DPPC or DPPG monolayer, the values of A_i

Received 2011-03-02, accepted 2012-02-13.
* Supported by the National Natural Science Foundation of China (20876047).
** To whom correspondence should be addressed. E-mail: zengzx@ecust.edu.cn

Table 1 Surface energy changes for the characteristic areas of phospholipid monolayer at 295 K

Molecule	Areas/nm^2·molecule^{-1}				Surface energy changes/J·molecule^{-1}			
	A_f	A_{LC}	A_t	A_i	$-\Delta E_{int}(A_f)$	$-\Delta E_{int}(A_{LC})$	$-\Delta E_{int}(A_t)$	$-\Delta E_{int}(A_i)$
DPPC	1.01	0.447	0.353	0.19	0	5.4×10^{-21}	10.4×10^{-21}	21.5×10^{-21}
DPPG	1.08	0.427	0.343	0.20	0	5.5×10^{-21}	9.7×10^{-21}	18.7×10^{-21}

and A_f can be obtained from experimental data in literature [15, 16]. The values of A_{LC} and A_t can be evaluated by regression [22]. All the values of the characteristic areas for DPPC or DPPG monolayer are shown in Table 1, where the molecular area approaching collapse is about 0.2 nm^2·molecule^{-1}.

3 MOLECULAR CONFORMATION

3.1 Energy changes of pure phospholipid monolayer

When a monolayer is compressed, the surface energy $E_{int}(A)$ is changed, which will cause conformational changes. The energy changes of the monolayer can be expressed as [24, 25]:

$$\Delta E_{con}(A) = \Delta E_{dis}(A) - \Delta E_{int}(A) - n\Delta E_{lip}(A) \quad (1)$$

where $\Delta E_{con}(A)$ is the conformation energy change between the current and initial states, $\Delta E_{int}(A)$ is the surface energy changes between the two states, $\Delta E_{lip}(A)$ is the energy change caused by one lipid molecule squeezed-out, n is the number of the molecules squeezed out, and $\Delta E_{dis}(A)$ is the dissipated energy of the system.

In this paper, we assume that no molecule is squeezed out and no energy is dissipated for pure phospholipids monolayer. Therefore, $n = 0$, $\Delta E_{lip}(A) = 0$ and $\Delta E_{dis}(A) = 0$, Eq. (1) is transformed to

$$\Delta E_{con}(A) = -\Delta E_{int}(A) \quad (2)$$

Equation (2) can be applied to any state of the monolayer during compressing. In the following work, it will be used to determine the molecular conformations of DPPC and DPPG at any state during compressing.

3.2 The surface energy change $\Delta E_{int}(A)$

The surface energy change between the current and initial states is expressed as

$$\Delta E_{int}(A) = E_{int}(A) - E_{int}(A_f) \quad (3)$$

where $E_{int}(A)$ and $E_{int}(A_f)$ represent the surface energy of the monolayer with molecular area A and A_f, respectively.

In the compressing process, the environment has to overcome the surface pressure that the monolayer bears, so $-\Delta E_{int}(A)$ can be obtained by integration from π-A isotherms:

$$-\Delta E_{int}(A) = E_{int}(A_f) - E_{int}(A) = \int_A^{A_f} \pi \mathrm{d}A \quad (4)$$

On the one hand, the experimental π-A isotherms can be obtained from references [15, 16], and the values of $-\Delta E_{int}(A)$ can be calculated by Simpson numerical integration. Plots of $-\Delta E_{int}(A)$ *vs*. A for DPPC and DPPG at 295 K are shown in Fig. 1.

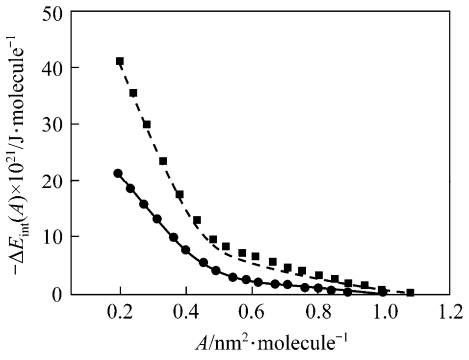

Figure 1 Surface energy changes of DPPC and DPPG at 295 K (dot: Simpson numerical integration; line: surface equation of state)
—●— DPPC; - - -■- - - DPPG

On the other hand, the surface equation of state proposed by Zeng *et al*. [22] can be applied to describe π-A isotherms, so Eq. (4) can also be transformed to:

$$-\Delta E_{int}(A) = \int_A^{A_f} \left[\frac{ZkT}{A} + \frac{\pi_{max} - ZkT/A}{1 + e^{\left(2\times\frac{A-A_{LC}}{A_{LC}-A_i}\right)}} \right] \mathrm{d}A \quad (5)$$

where π_{max} is defined as the maximum surface pressure that the monolayer can bear, and Z is the correction parameter. For phospholipid molecules, the value of Z is 1.

The relationships between $-\Delta E_{int}(A)$ and A for DPPC and DPPG at 295 K are illustrated in Fig. 1. The theoretical analysis results agree well with the experimental data. The absolute average deviation (AAD, %) is defined as

$$\mathrm{AAD} = \frac{1}{N}\left\{ \sum_{i=1}^{N} \frac{\left| \left[-\Delta E_{int}(A)\right]_{i,s} - \left[-\Delta E_{int}(A)\right]_{i,z} \right|}{\left| \left[-\Delta E_{int}(A)\right]_{i,s} \right|} \right\} \times 100\% \quad (6)$$

where N is the number of experimental points,

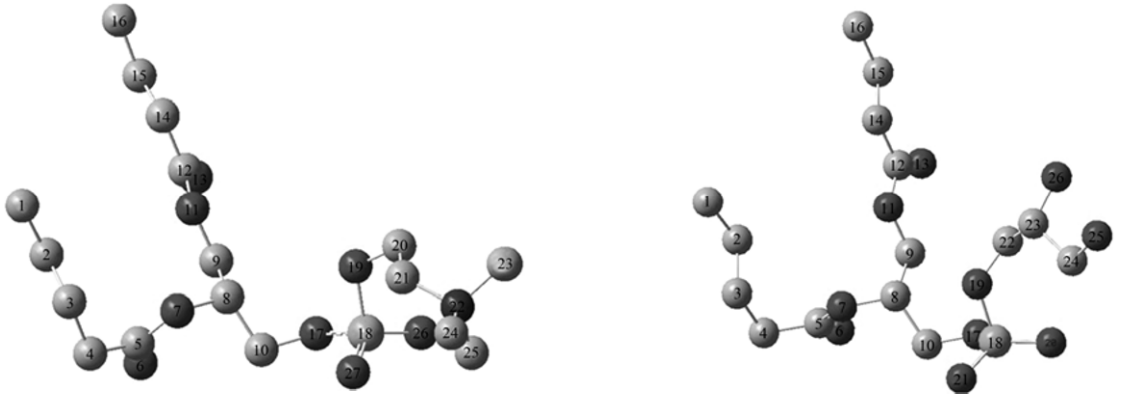

(a) DPPC (6,7,11,13,17,19,26,27: oxygen; 22: nitrogen; 18: phosphorus; 1−5,8−10,12,14−16,20,21,23−25: carbon)

(b) DPPG (6,7,11,13,17,19−21,25,26: oxygen; 18: phosphorus; 1−5,8−10,12,14−16,22−24: carbon)

Figure 2 The optimized conformation of DPPC and DPPG molecules at 295 K

$[-\Delta E_{\text{int}}(A)]_{i,\text{s}}$ is the value of $-\Delta E_{\text{int}}(A)$ calculated by Eq. (4) (Simpson numerical integration), and $[-\Delta E_{\text{int}}(A)]_{i,z}$ is that calculated by Eq. (5). The values of AAD for DPPC and DPPG are 9.53 and 10.96, respectively.

In this paper, Eq. (5) is used to predict the surface energy changes of the pure phospholipid (DPPC or DPPG) monolayer. The values of the surface energy changes corresponding to the characteristic areas are obtained and shown in Table 1.

3.3 Conformation energy change $\Delta E_{\text{con}}(A)$

According to the energy conservation law, when the temperature is constant, the internal energy change of the molecule, $\Delta E_{\text{i}}(A)$, is equal to the surface energy change. On the other hand, $\Delta E_{\text{i}}(A)$ can be expressed by the single point energy change. Thus $\Delta E_{\text{i}}(A)$ can be estimated by

$$-\Delta E_{\text{int}}(A) = \Delta E_{\text{i}}(A) = E_{\text{spe}}(A) - E_{\text{spe}}(A_{\text{f}}) \qquad (7)$$

where $E_{\text{spe}}(A)$ and $E_{\text{spe}}(A_{\text{f}})$ stand for the single point energy of the molecule with molecular area A and A_{f}, respectively. Substituting Eq. (2) into Eq. (7), we have

$$\Delta E_{\text{con}}(A) = E_{\text{spe}}(A) - E_{\text{spe}}(A_{\text{f}}) \qquad (8)$$

The conformation energy change $\Delta E_{\text{con}}(A)$ can be expressed by the single point energy change between current and initial states.

3.4 Initial molecular conformation and $E_{\text{spe}}(A_{\text{f}})$

The initial molecular conformations at 295 K and the values of $E_{\text{spe}}(A_{\text{f}})$ for DPPC and DPPG can be obtained through molecular conformation geometry optimization by Gaussian 98, where the B3LYP [26−28] exchange-correlation functional method together with the split-valence polarized 6−31G (d) are used. In the freedom state (A_{f}), the single point energy of the phospholipid molecule is the lowest, so the initial conformation can be determined with Gaussian 98 by searching for an equilibrium conformation. Fig. 2 illustrates the vital optimized conformations of DPPC and DPPG, where the bonds between C and H are omitted and the two palmitoyl chains are simplified to three methene groups.

The important conformational parameters for DPPC and DPPG in Fig. 2 are shown in Table 2. The values of $E_{\text{spe}}(A_{\text{f}})$ for DPPC and DPPG are -1.0833×10^{-14} and -1.0900×10^{-14} J·molecule^{-1}, respectively, which are about 10^7 times that of $-\Delta E_{\text{int}}(A)$ (shown in Table 1). Therefore, we can assume that the conformation energies of DPPC and DPPG change little during compressing.

3.5 Molecular conformational changes

When a monolayer is compressed, the conformational changes are complicated. For simplicity, only one bond is considered as the main contribution to the conformational changes of each lipid molecule. The assumptions are as follows.

(1) The conformation energy change is mainly caused by the rotation of one special bond which is indicated by the corresponding dihedral angle.

(2) The atoms of glycerol near the water surface are active. The rotated bond should be located near the water surface. The X-ray experiments performed on DPPC indicate that the phosphorus atom itself dose not rotate [29]. On the other hand, there are strong indications that the glycerol backbone itself undergoes a conformational change at the LE to solid phase transition [30]. Thus the atoms of glycerol near the surface are most active and play a key role in the compressing process.

(3) The rotation of bond is motivated by the hydrogen-bonding interaction between hydrophilic groups (glycerol and phosphate) and water molecules.

(4) The rotation of bond is inertial and follows the lowest cost path. In other words, when the conformation energy is changed by the same value, the slew range of the bond should be as small as possible.

Table 2 The optimized conformational parameters and $E_{spe}(A_f)$ of DPPC and DPPG at 295 K

Molecule	Bond lengths/nm	Bond angles/(°)	Dihedral angles/(°)	$E_{spe}(A_f)$/J·molecule^{-1}
DPPC	*B*(7,8) 0.146	*A*(5,7,8) 120.3	*D*(4,5,7,8) 178.6	-1.0833×10^{-14}
	B(8,10) 0.154	*A*(9,8,10) 112.2	*D*(9,8,10,17) 68.2	
	B(9,11) 0.145	*A*(8,9,11) 108.0	*D*(8,9,11,12) 173.9	
	B(10,17) 0.143	*A*(8,10,17) 109.3	*D*(8,10,17,18) 95.2	
	B(17,18) 0.163	*A*(10,17,18) 120.5	*D*(10,17,18,19) −86.9	
	B(18,19) 0.171	*A*(17,18,19) 97.9	*D*(17,18,19,20) −166.3	
	B(18,26) 0.150	*A*(17,18,26) 110.2	*D*(10,17,18,26) 161.9	
	B(18,27) 0.151	*A*(17,18,27) 111.3	*D*(10,17,18,27) 23.5	
DPPG	*B*(7,8) 0.146	*A*(5,7,8) 121.4	*D*(4,5,7,8) 178.0	-1.0900×10^{-14}
	B(8,10) 0.154	*A*(9,8,10) 112.3	*D*(9,8,10,17) 65.3	
	B(10,17) 0.142	*A*(8,10,17) 109.8	*D*(8,10,17,18) 85.0	
	B(17,18) 0.169	*A*(10,17,18) 118.3	*D*(10,17,18,20) 164.8	
	B(18,19) 0.169	*A*(17,18,19) 99.4	*D*(17,18,19, 22) −78.5	
	B(18,20) 0.150	*A*(17,18,20) 105.4	*D*(10,17,18,20) 164.8	
	B(18,21) 0.150	*A*(17,18,21) 108.7	*D*(10,17,18,21) 27.0	
	B(7,8) 0.146	*A*(5,7,8) 121.4	*D*(4,5,7,8) 178.0	

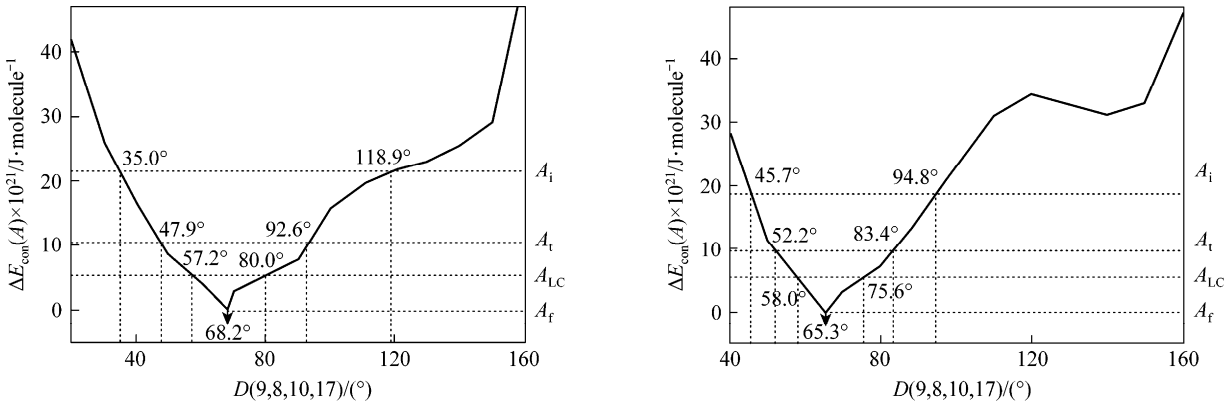

(a) DPPC (b) DPPG

Figure 3 The plots of $\Delta E_{con}(A)$ *vs.* D(9, 8, 10, 17) for DPPC and DPPG at 295 K

Based on the first three assumptions, the bonds *B*(8,10) and *B*(10,17) shown in Fig. 2 are considered as the most possible candidates to rotate during compressing. The corresponding dihedral angles are *D*(9,8,10,17) and *D*(8,10,17,18), respectively.

At the initial state, the values of *D*(9,8,10,17) and *D*(8,10,17,18) for DPPC (68.2° and 95.2°) and DPPG (65.3° and 85.0°) are shown in Figs. 3 and 4. When these dihedral angles are changed by a fixed value, the corresponding $E_{spe}(A)$ can be calculated by Guassian 98. By Eq. (8), the relationship between $\Delta E_{con}(A)$ and dihedral angle is established. Fig. 3 illustrates the plots of $\Delta E_{con}(A)$ *vs.* *D*(9,8,10,17) for DPPC and DPPG, and Fig. 4 illustrates their plots of $\Delta E_{con}(A)$ *vs.* *D*(8,10,17,18). According to Eq. (2) and the values of $-\Delta E_{int}(A)$ shown in Table 1, $\Delta E_{con}(A)$ with the characteristic areas (A_{LC}, A_t, A_i) can be calculated. The corresponding dihedral angles of DPPC and DPPG, as shown in Figs. 3 and 4, can be obtained from the plots of $\Delta E_{con}(A)$ *vs.* dihedral angle. In the compressing process, if the dihedral angle *D*(9,8,10,17) or *D*(8,10,17,18) rotates in clockwise direction (the values of the dihedral angle decrease), the values of $\Delta E_{con}(A)$ increase monotonically but irregularly. Since the plots of $-\Delta E_{int}(A)$ *vs.* *A* are monotonous (see Fig. 1) in the compressing process, the clockwise direction is more reasonable.

According to assumption (4), the slew range of the bond ($|\Delta D_A(9,8,10,17)|$ or $|\Delta D_A(8,10,17,18)|$) should be as small as possible, where $\Delta D_A(9,8,10,17)$ and $\Delta D_A(8,10,17,18)$ can be represented as

$$\Delta D_A(9,8,10,17) = D_A(9,8,10,17) - D_{A_f}(9,8,10,17) \quad (9)$$

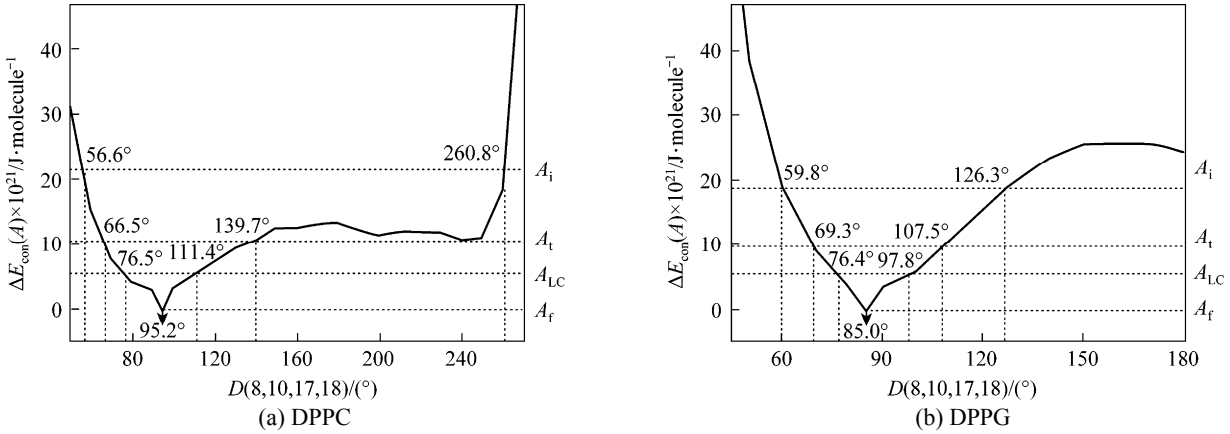

Figure 4 The plots of $\Delta E_{con}(A)$ *vs.* D(8, 10, 17, 18) for DPPC and DPPG at 295 K

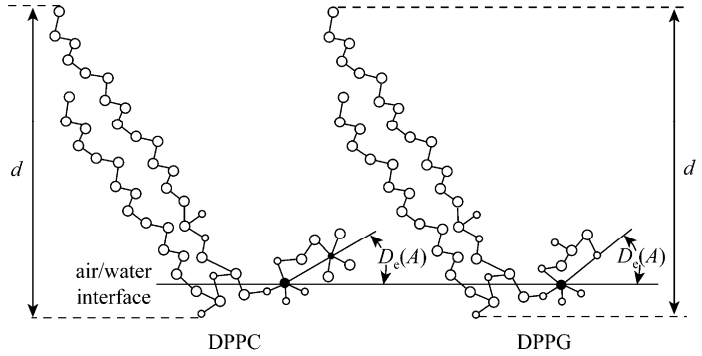

Figure 5 The orientations of DPPC and DPPG molecules at the air/water surface
○ oxygen; • nitrogen; ● phosphorus; ○ carbon

$$\Delta D_A(8,10,17,18) = D_A(8,10,17,18) - D_{A_f}(8,10,17,18) \quad (10)$$

where D_A and D_{A_f} are the dihedral angles of the molecules with molecular area A and A_f, respectively.

From Table 3, it is clear that the absolute values of $\Delta D_A(9,8,10,17)$ are generally less than that of $\Delta D_A(8,10,17,18)$, which means that conformatonal changes of DPPC and DPPG during compressing are mainly caused by the rotation of bond $B(8,10)$. This approximate description is one possible track, which takes account of the most active bond $B(8,10)$ near the surface, though there are still certain deviation.

Table 3 The values of $\Delta D_A(9,8,10,17)$ and $\Delta D_A(8,10,17,18)$ for DPPC and DPPG at 295 K

Dihedral/(°)	DPPC		DPPG	
	Clockwise	Anticlockwise	Clockwise	Anticlockwise
$\Delta D_{A_{LC}}(9,8,10,17)$	–11	11.8	–7.3	10.3
$\Delta D_{A_t}(9,8,10,17)$	–20.3	24.4	–13.1	18.1
$\Delta D_{A_i}(9,8,10,17)$	–33.2	50.7	–19.6	29.5
$\Delta D_{A_{LC}}(8,10,17,18)$	–18.7	16.2	–8.6	12.8
$\Delta D_{A_t}(8,10,17,18)$	–28.7	44.5	–15.7	22.5
$\Delta D_{A_i}(8,10,17,18)$	–38.6	165.6	–25.2	41.3

4 MOLECULAR ORIENTATION AT THE AIR/WATER SURFACE

The average area per molecule, A, is mainly determined by the orientation of molecules during compressing, so it is necessary to investigate the relationship between A and the molecular orientation of DPPC and DPPG at the air/water interface. According to the molecular orientation with different A, the compressing process can be divided into three stages: the tilt angle changing stage (from A_f to A_{LC}), the molecular overlapping stage (from A_{LC} to $2A_{LC}/3$) and the monolayer bending stage (from $2A_{LC}/3$ to A_i).

4.1 The tilt angle changing stage

The headgroup orientation of DPPC is generally referred to as the tilt angle of the phosphate-nitrogen dipole moment with respect to the surface [31]. Similarly, for DPPG, the angle between phosphate-oxygen vector and the monolayer surface stands for the headgroup orientation. The tilt angles $D_e(A)$, sketched in Fig. 5, change with different A. In this stage, with the

decrease of $D_e(A)$ caused by the rotation of bond $B(8,10)$, the molecular area of lipid is reduced dramatically from A_f to A_{LC}. A is the vertical projection area for the lipid molecule, which can be calculated based on Gaussian view [21]. The relationship between $D_e(A)$ and A for DPPC and DPPG are illustrated in Fig. 6. For DPPC, the values of $D_e(A_f)$ and $D_e(A_{LC})$ are 21.2° and −6.3°, respectively, and for DPPG, they are 59.9° and 21.7°, respectively.

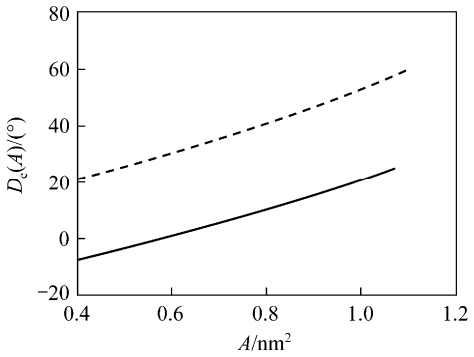

Figure 6 The plots of A *vs.* $D_e(A)$ calculated by Gaussian view at 295 K for DPPC and DPPG
—— DPPC; – – – DPPG

In addition, we have estimated the thickness of the simulated phospholipid monolayer d by measuring the length of the projection of the lipid molecule on the monolayer normal (see Fig. 5). As the monolayer reaches the completed LC state (A_{LC}), the increasing values of d_{DPPC} and d_{DPPG} are 0.52 nm and 0.61 nm, respectively. According to the neutron reflectivity measurements [4], the total monolayer thickness increases by 0.55 nm when compressing the DPPC-d_{75} monolayer from the LE phase to the condensed phase, which is very close to our simulated result.

4.2 The overlapping stage

For recent reports of the lipid molecular average area smaller than 0.4 nm^2·molecule^{-1} [15–20], Song *et al*. [32] suggested that it is a transition from monolayer to multilayer on acidic subphase. In this paper, a similar assumption is made.

In Table 1, the values of A_{LC} for DPPC and DPPG are both about 0.4 nm^2·molecule^{-1}, so A_{LC} is thought to be the minimum vertical projection area for the lipid molecule. When the monolayer is further compressed, some molecules are aggregated together and the overlapping phenomenon appears. The molecular area is replaced by the virtual molecular area to characterize the compressing process.

In order to depict the overlapping phenomenon, the overlapping coefficient, α, is defined:

$$\alpha = (n_o / n_T) \times 100\% \tag{11}$$

where n_o is the number of the overlapped molecules, and n_T is the total number of the molecules. Theoretically, there is an overlapped molecule for every three molecules, so the maximum value of α, α_{max}, is 33.3%. The virtual molecular area can be calculated by

$$A = A_{LC}(1-\alpha) \quad (2A_{LC}/3 \leqslant A \leqslant A_{LC}) \tag{12}$$

Based on Eq. (12), the values of α can be evaluated by

$$\alpha = 1 - A/A_{LC} \quad (2A_{LC}/3 \leqslant A \leqslant A_{LC}) \tag{13}$$

According to Eq. (13), the values of α for DPPC and DPPG at the transition state (A_t) are calculated to be 23.27% and 19.67%, respectively. Fig. 7 shows the molecular orientations of DPPC and DPPG with the molecular area, A_t.

4.3 The monolayer bending stage

As the monolayer is compressed, more and more

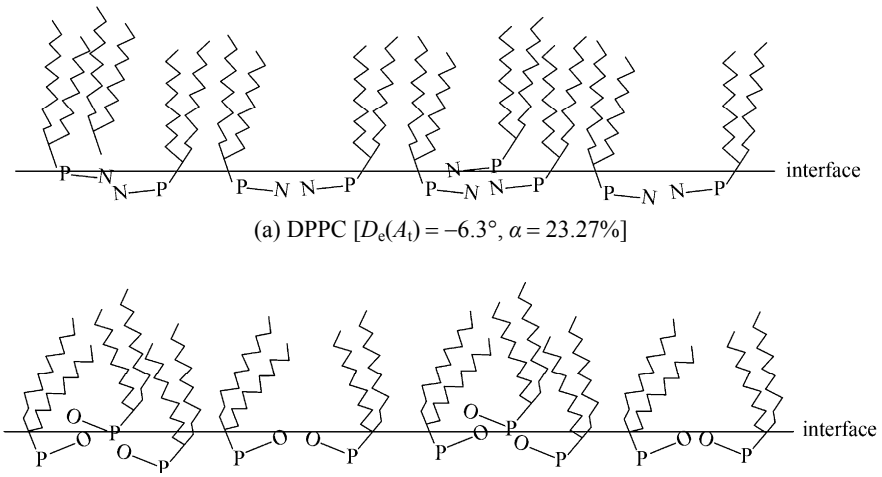

(a) DPPC [$D_e(A_t) = -6.3°$, $\alpha = 23.27\%$]

(b) DPPG [$D_e(A_t) = 21.7°$, $\alpha = 19.67\%$]

Figure 7 The molecular orientation of DPPC and DPPG at the transition state (A_t)
P—phosphate group; N—choline group; O—glycerol group

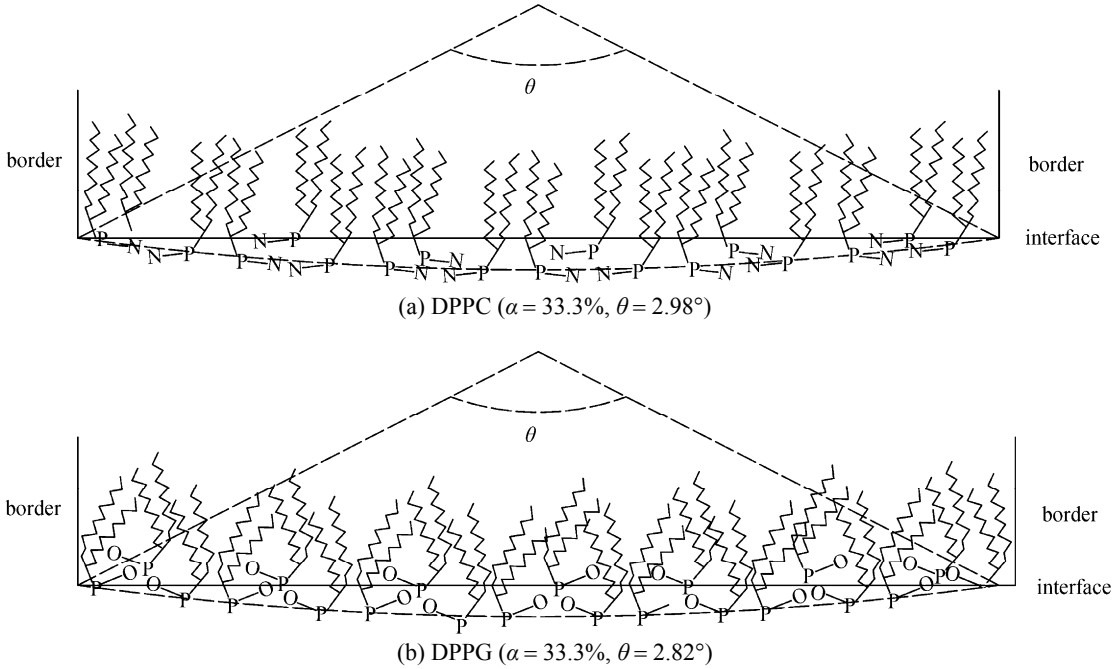

Figure 8 The molecular orientation of DPPC and DPPG at the collapse state (A_i)
P—phosphate group; N—choline group; O—glycerol group

molecules are aggregated together and α increases to the maximum, 33.3% at the area $2A_{LC}/3$. Then, according to Baoukina *et al*. [33], the monolayer begins to buckle and then collapses. When A is less than $2A_{LC}/3$, a parameter, θ, is proposed to characterize the bending degree of the monolayer. The relationship between A and θ is

$$\frac{2\sin(\theta/2)}{\theta}=\frac{A}{A_{LC}\left(1-\alpha_{max}\right)} \quad \left(A_i \leqslant A \leqslant 2A_{LC}/3\right) \tag{14}$$

Thus the virtual lipid area can be calculated by

$$A=4A_{LC}\frac{\sin(\theta/2)}{3\theta} \quad \left(A_i \leqslant A \leqslant 2A_{LC}/3\right) \tag{15}$$

Based on Eq. (15), the values of θ for DPPC and DPPG are 2.98° and 2.82° at the collapse state (A_i), respectively. Fig. 8 shows the orientations of DPPC and DPPG with the molecular area, A_i.

5 CONCLUSIONS

We performed computer simulations on the conformations of DPPC and DPPG in pure phospholipid monolayers at the air/water interface during compression. The simplified track of conformational change is characterized by the change of dihedral angle D(9,8,10,17). The conformations of phospholipid molecules at different states are simulated by Gaussian 98 software. In our simulations, the values of D(9,8,10,17) for DPPC and DPPG decrease by not more than 33.2° and 38.6°. The thickness of the simulated phospholipid monolayer is consistent with experimental result. According to molecular areas at different states, the molecular orientation in the compressing process can be divided into three stages: the tilt angle changing stage (from A_f to A_{LC}), the molecular overlapping stage (from A_{LC} to $2A_{LC}/3$) and the monolayer bending stage (from $2A_{LC}/3$ to A_i).

NOMENCLATURE

A	average area per molecule in the current state, $nm^2 \cdot molecule^{-1}$
AAD	absolute average deviation, %
D	dihedral angle of molecule, (°)
D_e	tilt angle, (°)
d	thickness of the simulated phospholipid monolayer, nm
E_{int}	surface energy, $J \cdot molecule^{-1}$
E_{spe}	single point energy, $J \cdot molecule^{-1}$
$\Delta E_{con}(A)$	conformation energy change between current and initial states, $J \cdot molecule^{-1}$
$\Delta E_{dis}(A)$	dissipated energy of the system, $J \cdot molecule^{-1}$
$\Delta E_i(A)$	internal energy change of molecule, $J \cdot molecule^{-1}$
$\Delta E_{int}(A)$	surface energy change between current and initial states, $J \cdot molecule^{-1}$
$\Delta E_{lip}(A)$	energy change caused by one lipid molecule squeezed-out, $J \cdot molecule^{-1}$
k	Boltzman constant ($= 1.380658\times10^{-23}$ $J \cdot K^{-1}$)
N	number of experimental points
n	number of the molecules squeezed out
n_o	number of the overlapped molecules
n_T	total number of molecules
T	temperature, K
Z	correction parameter
α	overlapping coefficient
θ	bending degree of monolayer, (°)
π	surface pressure, $mN \cdot m^{-1}$

Subscripts

DPPC	dipalmitoylphosphatidylcholine
DPPG	dipalmitoylphosphatidylglycerol
f	freedom state
i	collapse state
LC	liquid condensed state
max	maximum
s	Simpson numerical integration
t	transition state
z	surface equation of state

REFERENCES

1 Bi, X., Flach, C.R., Pérez-Gil, J., Plasencia, I., Andreu, D., Oliveira, E., Mendelsohn, R., "Secondary structure and lipid interactions of the *N*-terminal segment of pulmonary surfactant SP-C in Langmuir film: IR reflecton-adsorption spectroscopy and surface pressure studies", *Biochemistry*, **41** (26), 8385−8395 (2002).

2 Dieudonné, D., Mendelsohn, R., Farid, R.S., Flach, C.R., "Secondary structure in lung surfactant SP-B peptides: IR and CD studies of bulk and monolayer phases", *Biochim. Biophys. Acta*, **1511** (1), 99−112 (2001).

3 Veldhuizen, E.J.A., Haagasman, H.P., "Role of pulmonary surfactant components in surface film formation and dynamics", *Biochim. Biophys. Acta*, **1467** (2), 255−270 (2000).

4 Brumm, T., Naumann, C., Sackmann, E., Rennie, A.R., Thomas, R.K., Kanellas, D., Penfold, J., Bayed, T.M., "Conformational changes of the lecithin headgroup in monolayers at the air/water interface", *Eur. Biophys. J.*, **23** (4), 289−295 (1994).

5 Brezesinski, G., Thoma, M., Struth, B., Möhwald, H., "Structural changes of monolayers at the air/water interface contacted with *n*-alkanes", *J. Phys. Chem.*, **100** (8), 3126−3130 (1996).

6 Gericke, A., Moore, D.J., Erukulla, R.K., Bittman, R., Mendelsohn, R., "Partially deuterated phospholipids as IR structure probes of conformational order in bulk and monolayer phases", *J. Mol. Struct.*, **379** (1-3), 227−239 (1996).

7 Ma, G., Allen, H.C., "DPPC Langmuir monolayer at the air-water interface: probing the tail and head groups by vibrational sum frequency generation spectroscopy", *Langmuir*, **22** (12), 5341−5349 (2006).

8 Dominguez, H., Smondyrev, A.M., Berkowitz, M.L., "Computer simulations of phosphatidylcholine monolayers at air/water and CCl_4/water interfaces", *J. Phys. Chem. B*, **103** (44), 9582−9588 (1999).

9 Adhangale, P.S., Gaver, D.P., "Equation of state for a coarse-grained DPPC monolayer at the air/water interface", *Mol. Phys.*, **104** (19), 3011−3019 (2006).

10 Laing C., Baoukina S., Tieleman D.P., "Molecular dynamics study of the effect of cholesterol on the properties of lipid monolayers at low surface tensions", *Phys. Chem. Chem. Phys.*, **11** (12), 1916−1922 (2009).

11 Mohammad-Aghaie, D., Mace, E., Sennoga, C.A., Seddon, J.M., Bresme, F., "Molecular dynamics simulations of liquid condensed to liquid expanded transitions in DPPC monolayers", *J. Phys. Chem. B*, **114** (3), 1325−1335 (2010).

12 Shushkov, P., Tzvetanov, S., Velinova, M., Ivanova, A., Tadjer, A., "Structural aspects of lipid monolayers: computer simulation analyses", *Langmuir*, **26** (11), 8081−8092 (2010).

13 Zeng Z.X., Chen Q., Xue W.L., Nie F., "Surface equation of state for pure phospholipid monolayer at the air/water interface", *Chin. J. Chem. Eng.*, **12** (2), 263−266 (2004).

14 Krüger, P., Schalke, M., Wang, Z., Notter, R.H., Dluhy, R.A., Lösche, M., "Effect of hydrophobic surfactant peptides SP-B and SP-C on binary phospholipid monolayers. I. Fluorescence and dark-field microscopy", *Biophys. J.*, **77** (2), 903−914 (1999).

15 Taneva, S., Keough, K.M., "Pulmonary surfactant protein SP-B and SP-C in spread monolayers at the air-water interface: I. Monolayers of pulmonary surfactant protein SP-B and phospholipids", *Biophys. J.*, **66** (4), 1137−1148 (1994).

16 Taneva, S., Keough, K.M., "Pulmonary surfactant protein SP-B and SP-C in spread monolayers at the air-water interface: II. Monolayers of pulmonary surfactant protein SP-C and phospholipids", *Biophys. J.*, **66** (4), 1149−1157 (1994).

17 Taneva, S., Keough, K.M., "Pulmonary surfactant protein SP-B and SP-C in spread monolayers at the air-water interface: III. Proteins SP-B plus SP-C with phospholipids in spread monolayers", *Biophys. J.*, **66** (4), 1158−1166 (1994).

18 Wüstneck, N., Wüstneck, R., Fainerman, V.B., Miller, R., Pison, U., "Interfacial behaviour and mechanical properties of spread lung surfactant protein/lipid layers", *Colloids Surf. B*, **21** (1-3), 191−205 (2001).

19 Plasencia, I., Keough, K.M.W., Perez-Gil, J., "Interaction of the *N*-terminal segment of pulmonary surfactant protein SP-C with interfacial phospholipid films", *Biochim. Biophys. Acta*, **1713** (2), 118−128 (2005).

20 Biswas, N., Shanmukh, S., Waring, A.J., Walther, F., Wang, Z., Chang, Y., Notter, R.H., Dluhy, R.A., "Structure and properties of phospholipid–peptide monolayers containing monomeric SP-B1-25 I. Phases and morphology by epifluorescence microscopy", *Biophys. Chem.*, **113** (3), 223−232 (2005).

21 Frisch, M.J., Trucks, G.W., Schlegel, H.B., Scuseria, G.E., Robb, M.A., Cheeseman, J.R., Zakrzewski, V.G., Montgomery, J.A., Jr., Stratmann, R.E., Burant, J.C., Dapprich, S., Millam, J.M., Daniels, A.D., Kudin, K.N., Strain, M.C., Farkas, O., Tomasi, J., Barone, V., Cossi, M., Cammi, R., Mennucci, B., Pomelli, C., Adamo, C., Clifford, S., Ochterski, J., Petersson, G.A., Ayala, P.Y., Cui, Q., Morokuma, K., Malick, D.K., Rabuck, A.D., Raghavachari, K., Foresman, J.B., Cioslowski, J., Ortiz, J.V., Baboul, A.G., Stefanov, B.B., Liu, G., Liashenko, A., Piskorz, P., Komaromi, I., Gomperts, R., Martin, R.L., Fox, D.J., Keith, T., Al-Laham, M.A., Peng, C.Y., Nanayakkara, A., Challacombe, M., Gill, P.M.W., Johnson, B.G., Chen, W., Wong, M.W., Andres, J.L., Gonzalez, C., Head-Gordon, M., Replogle, E.S., Pople, J.A., Gaussian 98, Revision A. 7, Gaussian, Inc., Pittsburgh, PA (1998).

22 Zeng, Z.X., Li, D., Xue, W.L., Sun, L., "Structural models and surface equation of state for pulmonary surfactant monolayers", *Biophys. Chem.*, **131** (1-3), 88−95 (2007).

23 Pimthon, J., Willumeit, R., Lendlein, A., Hofmann, D., "All-atom molecular dynamics simulation studies of fully hydrated gel phase DPPG and DPPE bilayers", *J. Mol. Struct.*, **921** (1-3), 38−50 (2009).

24 Li, D., Zeng, Z.X., Xue, W.L., Yao, Y.L., "The model of the action mechanism of SP-C in the lung surfactant monolayers", *Colloids Surf. B*, **57** (1), 22−28 (2007).

25 Krüger, P., Baatz, J.E., Dluhy, R.A., Lösche, M., "Effects of hydrophobic surfactant protein SP-C on binary phospholipid monolayers. Molecular machinery at the air/water interface", *Biophys. Chem.*, **99** (3), 209−228 (2002).

26 Kohn, W., Sham, L.J., "Self-consistent equation including exchange and correlation effects", *Phys. Rev. A*, **140** (4), 1135−1138 (1965).

27 Levy, M., "Universal variational functionals of electron densities, first-order density matrices, and natural spin-orbitals and solution of the v-representation problem", *PNAS*, **76** (12), 6062−6065 (1979).

28 Becke, A.D., "Density-functional exchange-energy approximation with correct asymptotic behavior", *Phys. Rev. A*, **38** (6), 3098−3100 (1998).

29 Vakinin, D., Kjaer, K., Als-Nielsen, J., Lösche, M., "Structural properties of phosphatidylcholine in a monolayer at the air/water interface: Neutron reflection study and reexamination of X-ray reflection measurements", *Biophys. J.*, **59** (6), 1325−1332 (1991).

30 Bayerl, T.M., Thomas, R.K., Penfold, J., Rennie, A., Sackmann, E., "Specular reflection of neutrons at phospholipid monolayers. Changes of monolayer structure and headgroup hydration at the transition from the expanded to the condensed phase state", *Biophys. J.*, **57** (5), 1095−1098 (1990).

31 Hauser, H., Pascher, I., Pearson, R.H., Sundell, S., "Preferred conformation and molecular packing of phosphatidylethanolamine and phosphatidylcholine", *Biochim. Biophys. Acta*, **650** (1), 21−51 (1981).

32 Song, C.S., Ye, R.Q., Mu, B.Z, "Molecular behavior of a microbial lipopeptide monolayer at the air-water interface", *Colloids Surf. A*, **302** (1-3), 82−87 (2007).

33 Baoukina, S., Monticelli, L., Risselada, H.J., Marrink, S.J., Tieleman, D.P., "The molecular mechanism of lipid monolayer collapse", *PNAS*, **105** (31), 10803−10808 (2008).